Transactions, SMiRT-22
San Francisco, California, USA - August 18-23, 2013
Division V

DEFINITION OF STATIC LOAD CASES EQUIVALENT TO THE SEISMIC ACTION USING PEAK RESPONSE HYPER-ELLIPSOID ENVELOPES: THEORETICAL FORMULATION, ALGORITHMIC ASPECTS AND APPLICATION TO A NPP BUILDING

Quang Sang Nguyen[1], Silvano Erlicher[2], and François Martin[3]

[1] Engineer, Egis Industries, Montreuil, France (quang-sang.nguyen@egis.fr)
[2] Senior Engineer, PhD, Egis Industries, Montreuil, France (silvano.erlicher@egis.fr)
[3] Senior Engineer, Egis Industries, Montreuil, France (francois.martin@egis.fr)

ABSTRACT

Earthquake analysis plays an important role in Nuclear Power Plant (NPP) buildings design. Among the existing seismic analysis methods, the response spectrum method is one of the most used in this domain. Different variants exist, associated with different ways of accounting for the simultaneity of peak responses of physically distinct quantities. Peak simultaneity can be rigorously treated by the peak response hyper-ellipsoid envelopes (Menun and Der Kiureghian, 2000a,b). Another method to represent the seismic action is the so-called "equivalent static method" (ASCE, 2009). Nguyen et al. (2012) proposed a novel procedure for the definition of equivalent static loads, based on the notion of peak response hyper-ellipsoid envelope. In the present paper, this definition of equivalent static loads related to the peak response hyper-ellipsoid envelope is recalled and studied in-depth.

Several discretization algorithms of the hyper-ellipsoid envelope are also proposed. A "classical" procedure, (Leblond, 1980, Vézin et al., 2007), consists in approximating the hyper-ellipsoid by an enveloping polyhedron. An improved version of this procedure is proposed here by reducing the distance between this polyhedron and the hyper-ellipsoid surface. Moreover, a second procedure is proposed where the hyper-ellipsoid is approximated by calculating the intersection of two parallelepipeds enveloping it.

The novel methods for the definition of equivalent static loads and for the approximation of the hyper-ellipsoid envelope are finally applied to a representative NPP building. The obtained results (in particular, the total volume of the computed steel reinforcement) are compared with those obtained by several classical variants of the response spectrum method.

1. PEAK RESPONSE ENVELOPE

Let us consider an N-degree-of-freedom linear and classically damped structure, for which N real eigenmodes can be calculated. For seismic applications, only $n \leq N$ modes are usually retained, by either guarantying that the sum of effective masses of the n modes is high enough or introducing a pseudo-mode. The seismic effects are estimated by considering three earthquakes (represented by pseudo-acceleration spectra), one per direction ($k = x, y, z$). For an earthquake in direction k, the 3N-components displacement vector $\underline{u}_k(t)$ can be written as a linear combination of the modal peak displacement vectors $\underline{U}_{i,k} = R_{i,k}\gamma_{i,k}\underline{\phi}_i$:

$$\underline{u}_k(t) = \sum_i r_{i,k}(t)\,\gamma_{i,k}\underline{\phi}_i = \sum_i \alpha_{i,k}(t)\,R_{i,k}\gamma_{i,k}\underline{\phi}_i = \sum_i \alpha_{i,k}(t)\underline{U}_{i,k} \text{ with } -1 \leq \alpha_{i,k}(t) = r_{i,k}(t)/R_{i,k} \leq 1 \quad (1)$$

where $\underline{\phi}_i$ is the 3N-components eigenvector for mode i; $\gamma_{i,k} = \left(\underline{\phi}_i^T \underline{\underline{M}}\, \Delta_k\right)/\left(\underline{\phi}_i^T \underline{\underline{M}}\, \underline{\phi}_i\right)$ is the participation factor for mode i and the earthquake direction k; $R_{i,k} = \max_t\left|r_{i,k}(t)\right| = S_{d,k}(\omega_i, \xi_i)$ is the maximum displacement amplitude; $S_{d,k}(\omega_i,\xi_i)$ is the value read in the displacement spectrum corresponding to the pulsation ω_i and the damping ξ_i; $\underline{\underline{M}}$ is the structure mass matrix; $\Delta_k$is the earthquake direction vector; the time-function $r_{i,k}(t)$ is the solution of dynamics equation of the single-degree-of-freedom oscillator representing the mode *i* undergoing the ground acceleration $\ddot{s}_{g,k}(t)$ associated with $S_{d,k}(\omega_i,\xi_i)$. The *linear combination coefficient* $\alpha_{i,k}(t)$ is the ratio between the displacement $r_{i,k}(t)$ and its maximum value $R_{i,k}$.

The total displacement due to the earthquake in the three directions reads:

$$\underline{u}(t) = \sum_k \underline{u}_k(t) = \sum_k \sum_i \alpha_{i,k}(t)\underline{U}_{i,k} \tag{2}$$

1.1. Hyper-ellipsoid of linear combination coefficients (α-ellipsoid): case of a single seismic response

Let us consider a seismic response $f(t)$, e.g. a displacement, an axial force, a moment, etc. in a node, section or element of the structure. By virtue of linearity, one can always find a vector $\underline{d}$ such that:

$$f(t) = \underline{d}^T\underline{u}(t) = \sum_k \sum_i \alpha_{i,k}(t)\underline{d}^T\underline{U}_{i,k} = \sum_k \sum_i \alpha_{i,k}(t)F_{i,k} = \sum_k f_k(t) \tag{3}$$

where $F_{i,k} = \underline{d}^T\underline{U}_{i,k}$ is the value of the seismic response corresponding to the peak displacement vector $\underline{U}_{i,k}$ for the mode *i* and direction *k*. Equation 3 shows that at any time *t*, a seismic response $f(t)$ can also be written as the sum of three contributions $f_k(t)$, one per each earthquake direction k.

In the sense of probability, the maximum value of $f_k(t)$ can be estimated using the Complete Quadratic Combination-CQC of modal peaks (Der Kiureghian, 1979) $F_k^{CQC} = \sqrt{\sum_{ij}\rho_{ij}F_{i,k}F_{j,k}}$, where $\rho_{ij}$is the modal cross-correlation coefficient between modes *i* and *j*:

$$\rho_{ij} = \frac{8\sqrt{\xi_i\xi_j\omega_i\omega_j}(\omega_i\xi_i+\omega_j\xi_j)\omega_i\omega_j}{\left(\omega_i^2-\omega_j^2\right)^2+4\xi_i\xi_j\omega_i\omega_j\left(\omega_i^2+\omega_j^2\right)+4\omega_i^2\omega_j^2\left(\xi_i^2+\xi_j^2\right)} \tag{4}$$

Thus, in order for a linear combination $f_k(t)$ of modal responses to be probable, it must fulfill the condition:

$$f_k(t) = \sum_i \alpha_{i,k}(t)F_{i,k} \leq F_k^{CQC} \quad \text{or} \quad \underline{\alpha}_k^T(t)\underline{F}_k \leq \sqrt{\underline{F}_k^T\,\underline{\underline{H}}\,\underline{F}_k} \tag{5a \& 5b}$$

where $\underline{\alpha}_k(t) = \left[\alpha_{1,k}(t),\alpha_{2,k}(t),\dots,\alpha_{n,k}(t)\right]^T$ is the vector of the combination coefficients for all modes and direction k, $\underline{F}_k = \left[F_{1,k},F_{2,k},\dots,F_{n,k}\right]^T$ is the vector of the modal force peaks and $\underline{\underline{H}} = \left[\rho_{ij}\right]$ is the $n\times n$ matrix of the modal correlation coefficients. The inequalities in Equations 5a,b can be extended to the case of three earthquake directions using a quadratic combination of F_k^{CQC} (e.g. Menun and Der Kiureghian, 2000a):

$$f(t) = \sum_k f_k(t) = \sum_k \sum_i \alpha_{i,k}(t)F_{i,k} \leq F^{CQC} = \sqrt{\sum_k\left(F_k^{CQC}\right)^2} = \sqrt{\sum_k \sum_{ij}\rho_{ij}F_{i,k}F_{j,k}} \tag{6a}$$

or

$$\underline{\alpha}(t)^T\underline{F} \leq \sqrt{\underline{F}^T\,\underline{\underline{\tilde{H}}}\,\underline{F}}, \text{ with } \underline{\alpha} = \left[\underline{\alpha}_x^T,\underline{\alpha}_y^T,\underline{\alpha}_z^T\right]^T, \underline{F} = \left[\underline{F}_x^T,\underline{F}_y^T,\underline{F}_z^T\right]^T \text{ and } \underline{\underline{\tilde{H}}} = \text{diag}\left[\underline{\underline{H}},\underline{\underline{H}},\underline{\underline{H}}\right] \tag{6b}$$

From Equations 5b and 6b, supposing that the matrix $\underline{\underline{H}}$ is invertible, one can prove that (Martin, 2004):

$$\underline{\alpha}_k^T\,\underline{\underline{H}}^{-1}\underline{\alpha}_k \leq 1 \quad \text{and} \quad \underline{\alpha}^T\,\underline{\underline{\tilde{H}}}^{-1}\underline{\alpha} \leq 1 \tag{7a \& 7b}$$

Equations 7a,b mean that the coefficients $\underline{\alpha_k}$ and $\underline{\alpha}$ define probable combinations of peak responses when they belong to a n and $3n$-dimension hyper-ellipsoid (named α_k-ellipsoid and α-ellipsoid), respectively. In other words, each point inside or on the boundary of the α-ellipsoid corresponds to a probable state of the structure during the earthquake.

1.2. α-ellipsoid and f-ellipsoid: case of n_r different seismic responses

Let $\underline{x}_k(t) = \left[f_{1,k}(t), f_{2,k}(t), \dots, f_{n_r,k}(t)\right]^T$ be a vector of n_r simultaneous seismic responses (e.g. normal effort and moments in a beam section, membrane and bending efforts in a shell element,…) due to an earthquake in direction k, and let $\underline{\underline{R}}_k = \left[\underline{F}_{1,k}, \underline{F}_{2,k}, \dots, \underline{F}_{n_r,k}\right]$ be a $n \times n_r$ matrix whose columns $\underline{F}_{r,k} = \left[F_{r,1,k}, F_{r,2,k}, \dots, F_{r,n,k}\right]^T$ are the vectors of peak modal values of the responses $f_{r,k}(t)$. By virtue of structural linearity, one has: $\underline{x}_k = \underline{\underline{R}}_k^T \, \underline{\alpha}_k$. Moreover, supposing that the matrix $\underline{\underline{H}}$ is invertible, one can prove that:

$$\underline{x}_k^T \, \underline{\underline{X}}_k^{-1} \underline{x}_k = \underline{\alpha}_k^T \, \underline{\underline{H}}^{-1} \underline{\alpha}_k \leq 1 \qquad \text{(8a)}$$

where $\underline{\underline{X}}_k = \underline{\underline{R}}_k^T \underline{\underline{H}} \, \underline{\underline{R}}_k$ ($n_r \times n_r$ matrix). The inequality follows from Equation 7a. In the case of three earthquake directions, one can also prove that:

$$\underline{x}^T \, \underline{\underline{X}}^{-1} \underline{x} = \underline{\alpha}^T \, \underline{\underline{\tilde{H}}}^{-1} \underline{\alpha} \leq 1 \qquad \text{(8b)}$$

where $\underline{\underline{X}} = \sum_k \underline{\underline{X}}_k$ and $\underline{x} = \sum_k \underline{x}_k$. Equations 8a,b considered as identities, define two hyper-ellipsoids of dimension n_r, that we name f_k*-ellipsoid* and *f-ellipsoid*, respectively. Each point inside or on the boundary of *f-ellipsoid* corresponds to a probable combination of the n_r simultaneous seismic responses $f_1(t), f_2(t), \dots, f_{n_r}(t)$. Equation 8b implies that a point $\underline{x}$ of the *f-ellipsoid* corresponds to one and only one point $\underline{\alpha}$ of the α-ellipsoid.

2. DISCRETIZATION OF HYPER-ELLIPSOID ENVELOPES

For practical application purposes, a finite number of probable combinations of simultaneous seismic responses must be considered for the seismic analysis. They correspond to a finite number of points on the *f-ellipsoid* surface. Several discretization methods exist, in particular the one provided in ASCE (2009). Two new approaches, efficient and easy to implement, are presented hereinafter.

2.1. Polyhedron envelope

The first approach proposed by Leblond (1980) for cases n_r=2 and n_r=3 consists in replacing the hyper-ellipsoid by a polyhedron enveloping the hyper-ellipsoid. The extension of Leblond's approach to the general case with n_r>3 dimensions was presented by Vézin et al. (2007), and discussed by Nguyen et al. (2012). The use of this polyhedron leads to conservative results since the polyhedron is "larger" than the envelope. The original procedure of Vézin et al. (2007) is recalled hereinafter (steps 1 to 5, see also Figure 1). An improvement (from step 3) is also proposed leading to a reduction of the margin between the hyper-ellipsoid and the polyhedron:

Step 1: Diagonalize the $n_r \times n_r$ matrix $\underline{\underline{X}}$ defining the *f-ellipsoid* (Section 1.2), i.e. find the diagonal matrix $\underline{\underline{Y}} = diag\left(\lambda_1, \lambda_2, \dots, \lambda_{n_r}\right)$ and the matrix $\underline{\underline{D}}$ such that $\underline{\underline{X}} = \underline{\underline{D}}^T \underline{\underline{Y}} \, \underline{\underline{D}}$. Notice that $\lambda_1, \lambda_2, \dots, \lambda_{n_r}$ are the eigenvalues of $\underline{\underline{X}}$, while $\underline{\underline{D}}$ is the $n_r \times n_r$ matrix whose columns are the eigenvectors of $\underline{\underline{X}}$.

Step 2: Transform the *f-ellipsoid* into a hyper-sphere with unit radius by the affinity $u : \Re^{n_r} \mapsto \Re^{n_r}$ such that $u : \underline{S} \mapsto \underline{V} = \underline{\underline{Y}}^{-1/2} . \underline{S}$

Step 3: Define a polyhedron enveloping a unit hyper-sphere following two approaches:

A) $\boldsymbol{n_r \times 2^{n_r}}$ **points** (Vézin et al. 2007): $\underline{V}_j^{(i)} = [\pm a, \pm a, \dots, \pm 1, \dots, \pm a]^T$, with $j = 1, \dots, 2^{n_r}$, $i = 1, \dots, n_r$ and $a = \sqrt{2} - 1 \approx 0.42$ (the component of $\underline{V}_j^{(i)}$ equal to plus or minus 1 is the *i-th*).

B) $\boldsymbol{(n_r - 1) \times n_r \times 2^{n_r}}$ **points:** In order to improve the accuracy, each one of the points $\underline{V}_j^{(i)} = [\pm a, \pm a, \dots, \pm 1, \dots, \pm a]^T$ can be replaced by *(nr -1)* points $\underline{W}_{j,m}^{(i)}$ with $m = 1, \dots n_r - 1$, which give a finer approximation. Hence, the new enveloping polyhedron has $(n_r - 1) \times n_r \times 2^{n_r}$ points (see Table 1):

$$\underline{W}_{j,1}^{(i)} = [\pm a, \pm \beta a, \pm \beta a, \pm \beta a, \dots, \pm 1, \dots, \pm \beta a]^T$$
$$\underline{W}_{j,2}^{(i)} = [\pm \beta a, \pm a, \pm \beta a, \pm \beta a, \dots, \pm 1, \dots, \pm \beta a]^T$$
$$\dots$$
$$\underline{W}_{j,n_r-1}^{(i)} = [\pm \beta a, \pm \beta a, \pm \beta a, \pm \beta a, \dots, \pm 1, \dots, \pm a]^T$$

where $j = 1, \dots, 2^{n_r}$, $i = 1, \dots, n_r$, $a = \sqrt{2} - 1 \approx 0.42$ and β is a positive coefficient less than 1. The recommended values of β are provided in Table 2.These values of β are calculated by an iterative procedure reducing step by step the distance between each one of the 2^{n_r} hyper-planes defined by the $(n_r - 1) \times n_r$ points $\underline{W}_{j,1}^{(1)}, \underline{W}_{j,1}^{(2)}, \dots, \underline{W}_{j,1}^{(n)}, \dots, \underline{W}_{j,(n_r-1)}^{(n_r)} (j = 1, \dots, 2^{n_r})$ and the reference point $\underline{O}$, until this distance is equal or lightly greater than 1 (Table 3).

Step 4: Transform the polyhedron enveloping the hyper-sphere (Step 3) into a polyhedron enveloping the hyper-ellipsoid in the diagonalization reference:

A) $\underline{S}_j^{(i)} = \underline{\underline{Y}}^{1/2} . \underline{V}_j^{(i)} = \left[\pm a\sqrt{\lambda_1}, \pm a\sqrt{\lambda_2}, \dots, \pm\sqrt{\lambda_i}, \dots, \pm a\sqrt{\lambda_{n_r}}\right]^T$

B) $\underline{S'}_{j,m}^{(i)} = \underline{\underline{Y}}^{1/2} . \underline{W}_{j,m}^{(i)} = \left[\pm \beta a\sqrt{\lambda_1}, \pm \beta a\sqrt{\lambda_2}, \dots, \pm\sqrt{\lambda_i}, \dots, \pm a\sqrt{\lambda_m}, \dots, \pm \beta a\sqrt{\lambda_{n_r}}\right]^T$

Step 5: Transform the polyhedron defined at Step 4 into a polyhedron enveloping the hyper-ellipsoid in the original reference: $\underline{x}_j^{(i)} = \underline{\underline{D}}^T \underline{S}_j^{(i)}$ (approach A) or $\underline{x}_{j,m}^{(i)} = \underline{\underline{D}}^T \underline{S'}_{j,m}^{(i)}$ (approach B).

Table 1: Number of retained discretization points for both discretization approaches (A and B)

	n_r	2	3	4	5	6	7	8
A	$n_r \times 2^{n_r}$	8	24	64	160	384	896	2048
B	$(n_r - 1)n_r \times 2^{n_r}$	8	48	192	640	1920	5376	14336

Table 2: Recommended values of β

n_r	2	3	4	5	6	7	8
β	1	0.7677	0.7071	0.6614	0.6249	0.5946	0.5690

Table 3: Distances from the reference point (the origin $\underline{O}$) to the hyper-planes defined by the points $\underline{V}_j^{(1)}, \underline{V}_j^{(2)}, \dots, \underline{V}_j^{(n_r)}$ and $\underline{W}_{j,1}^{(1)}, \underline{W}_{j,1}^{(2)}, \dots, \underline{W}_{j,1}^{(n)}, \dots, \underline{W}_{j,(n_r-1)}^{(n_r)}$ (calculated with β in Table 2)

	n_r	2	3	4	5	6	7	8
A	$d(\underline{O}, Hyper - plane\ \underline{V}_j^{(i)})$	1	1.06	1.12	1.19	1.25	1.32	1.38
B	$d(\underline{O}, Hyper - plane\ \underline{W}_{j,m}^{(i)})$	1	1.00008	1.000008	1.000005	1.00001	1.00001	1.00001

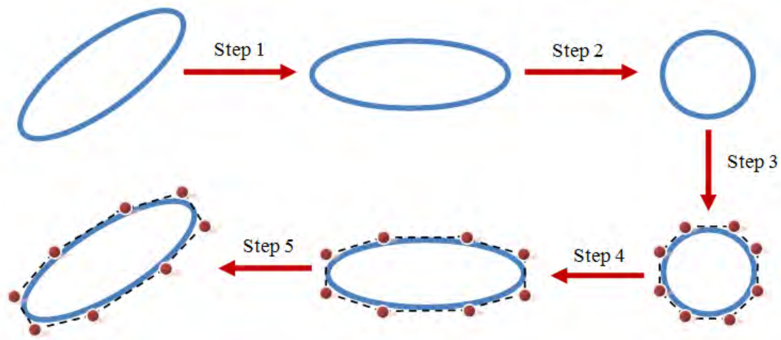

Figure 1. Discretization of a hyper-ellipsoid by an enveloping polyhedron (case $n_r = 2$).

The difference between approaches A and B (see step 3) can be clarified by comparing the distances from each one of the 2^{n_r} hyper-planes defined by the n_r points $\underline{V}_j^{(1)}, \underline{V}_j^{(2)}, \ldots, \underline{V}_j^{(n_r)}$ (j=1,…, 2^{n_r}) to the origin (approach A) and from each one of the 2^{n_r} hyper-planes defined by the $(n_r - 1) \times n_r$ points $\underline{W}_{j,1}^{(1)}, \underline{W}_{j,1}^{(2)}, \ldots, \underline{W}_{j,1}^{(n)}, \ldots, \underline{W}_{j,(n-1)}^{(n_r)} (j = 1, \ldots, 2^{n_r})$ to the origin (approach B), see Table 3. The distances $d\left(\underline{O}, Hyper - plane\ \underline{V}_j^{(i)}\right)$ are greater than $d\left(\underline{O}, Hyper - plane\ \underline{W}_{j,m}^{(i)}\right)$. This means that the use of $(n_r - 1) \times n_r \times 2^{n_r}$ points $\underline{W}_{j,m}^{(i)}$ permits a finer approximation of the hyper-ellipsoid. However, the number of points of this approach B is greater than in the basic algorithm (approach A) (Table 2).

2.2. Intersection between two parallelepiped envelopes

The second approach consists in finding the intersection between two parallelepiped envelopes of the hyper-ellipsoid. As already seen in Equations 5a and 6a, each seismic response parameter is limited by a value defined by the CQC: $f_i \le F^{(i,CQC)}$ $(i = 1, \ldots, n_r)$. As a result, the hyper-ellipsoid envelope of the peak of response parameters is enveloped by a “CQC-parallelepiped” defined by 2^{n_r} vertices with coordinates: $\pm F^{(1,CQC)}, \pm F^{(2,CQC)}, \pm F^{(3,CQC)} \pm F^{(4,CQC)}, \ldots, \pm F^{(n_r,CQC)}$ (see Figure 2).

Besides, there is a second parallelepiped envelope of the hyper-ellipsoid, each axis of which corresponds to a principal axis of the hyper-ellipsoid (Figure 2). The intersection points between these two parallelepipeds can be found by solving a number of systems of linear equations. Thus, the implementation of this approach is straightforward. Some results of this approach will be presented in Section 4.

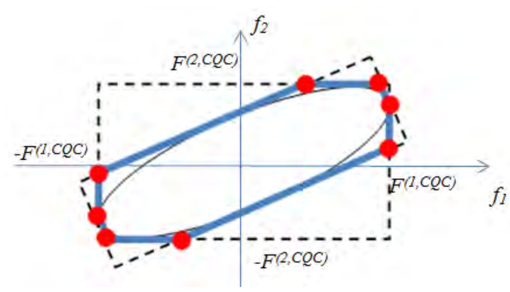

Figure 2. Intersection of two rectangles enveloping the elliptical peak response envelope (case $n_r = 2$).

3. DEFINITION OF EQUIVALENT STATIC LOADS

For some applications, it may be useful to represent the seismic action on a structure by one (or several) equivalent static load field(s), usually defined at each node of the structural model as the product between the nodal mass and suitable nodal accelerations. From Equations 1 and 2, one can define the displacement $u_x^l(t)$, the pseudo-acceleration $a_x^l(t)$ and the force $q_x^l(t)$ in the direction x for the node l of the structure:

$$u_x^l(t) = \sum_k \sum_i \alpha_{i,k}(t) U_{i,k,x}^l \tag{9a}$$

$$a_x^l(t) = \sum_k \sum_i \alpha_{i,k}(t) \omega_i^2 U_{i,k,x}^l = \sum_k \sum_i \alpha_{i,k}(t) A_{i,k,x}^l \tag{9b}$$

$$q_x^l(t) = \sum_k \sum_i \alpha_{i,k}(t) m^l \omega_i^2 U_{i,k,x}^l = \sum_k \sum_i \alpha_{i,k}(t) Q_{i,k,x}^l \tag{9c}$$

where $U_{i,k,x}^l, A_{i,k,x}^l$ and $Q_{i,k,x}^l$ are respectively the peak displacement of node l and the corresponding pseudo-acceleration and force for mode i, in the direction x and due to the earthquake direction k; m^l is the mass of the node l. Analogous expressions can be written for directions y and z, leading to the following nodal force field at the generic time t:

$$\underline{q}(t) = \left[\underline{q}_x(t), \underline{q}_y(t), \underline{q}_z(t)\right] = \left[q_x^1(t), \dots, q_x^N(t), q_y^1(t), \dots, q_y^N(t), q_z^1(t), \dots, q_z^N(t)\right]^T = \sum_k \sum_i \alpha_{i,k}(t) \underline{Q}_{i,k} \tag{10}$$

where $\underline{Q}_{i,k} = \left[Q_{i,k,x}^1, Q_{i,k,x}^2, \dots, Q_{i,k,x}^N, Q_{i,k,y}^1, \dots, Q_{i,k,y}^N, Q_{i,k,z}^1, Q_{i,k,z}^2, \dots, Q_{i,k,z}^N\right]^T$ is the vector of the modal peak forces defined in Equation 9c.

In general, the combination coefficients $\alpha_{i,k}$ are not known. However, if a dominant mode exist for each direction k (we can indicate these three modes with the indices (1,x), (1,y) and (1,z)), one has $\underline{q}_k(t) \approx \underline{Q}_{1,k}$. The dominant mode is considered representative for the earthquake in direction k ($\alpha_{1,k} \approx 1$). An alternative procedure is based on the use of the Complete Quadratic Combination: for each earthquake direction k, the force field $\underline{q}_k = \left[q_k^{1,CQC}, q_k^{2,CQC}, \dots, q_k^{N,CQC}\right]^T$ is defined, with $q_k^{l,CQC} = \sqrt{\sum_{ij} \rho_{ij} Q_{i,k,k}^l Q_{j,k,k}^l} = m^l \sqrt{\sum_{ij} \rho_{ij} A_{i,k,k}^l A_{j,k,k}^l}$. The sign of $q_k^{l,CQC}$ is associated with the sign of the first dominant mode. In these two approaches, the Newmark's rule is used to combine the force fields associated with different earthquake directions $\underline{q}_k$, to define $\underline{q}$. In these cases, the linear combination in Equation 10 is not used.

In this Section, a procedure is proposed to define the $\alpha_{i,k}$ coefficient using the *α-ellipsoid and* a particular case of *f-ellipsoid*. First, observe that at a given time *t*, the vector of nodal forces $\underline{q}(t)$ in Equation 10 depends on the vector $\underline{\alpha}(t)$ and corresponds to one static load case. Moreover, it has been previously proven that the *locus* of probable values of the combination coefficients $\alpha(t)$ is the *α-ellipsoid* defined by Equation 7b. For n modes, the *α-ellipsoid* has dimension 3n. Its polyhedral envelope would have either $3n \times 2^{3n}$ points (approach A) or $(3n-1) \times 3n \times 2^{3n}$ (approach B) (see Section 2.1). These numbers are too large for practical calculations, especially for multi-modal structures, where the number n of significant modes can be very important. Actually, instead of finding all the points $\underline{\alpha}$ approximating the *α-ellipsoid* (in order to define all force fields $\underline{q}(t)$), a preliminary selection of the *most important ones* (according to some engineering criteria) could be performed.

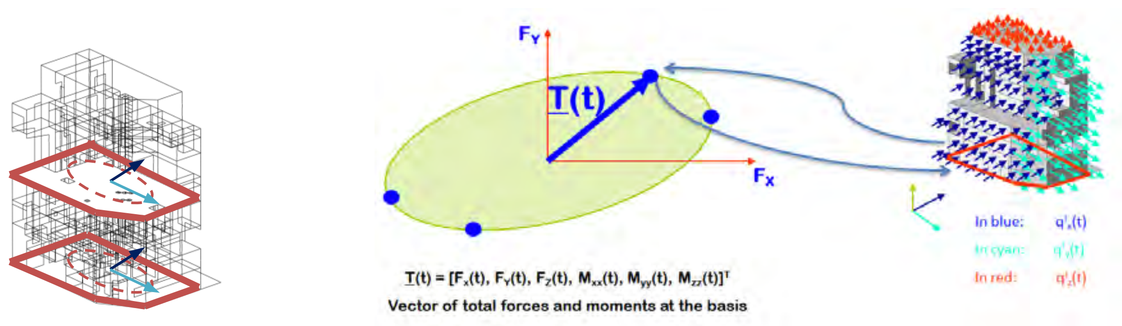

Figure 3. Selection of the most important points $\underline{\alpha}$ according to the total forces and moment at the basis

For instance, it is possible to look for the 6 points $\underline{\alpha}$ belonging to the α-ellipsoid *and* maximizing the total shear seismic forces $F_x(t), F_y(t), F_z(t)$ and moments $M_{xx}(t), M_{yy}(t), M_{zz}(t)$ at the basis of the building (or at another given level of the structure). However, these six cases do not account for coupling effects between the six generalized forces. Actually, *a complete description of probable seismic forces at the base of the building is provided by the corresponding 6D hyper-ellipsoid (named here T-ellipsoid)*: each point $\underline{T} = [F_x, F_y, F_z, M_{xx}, M_{yy}, M_{zz}]^T$ of this *T-ellipsoid* represents one probable combination of the total forces and moments at the base. The *T-ellipsoid* is a particular case of *f-ellipsoid* (section 1.2). Hence, it is proposed to look for the points $\underline{\alpha}$ fulfilling Equation 7b *and* such that the corresponding vector of total forces and moments at the base belongs to the *T-ellipsoid*. In practice, the *T-ellipsoid* can be approximated by a 6D-polyhedron with 6x2^6 = 384 vertices and the number of points $\underline{\alpha}$ is 384 (or 5x6x2^6 = 1920 points for approach B). An analytical procedure to calculate $\underline{\alpha}$ for a given point $\underline{T}$ is proposed hereafter. First, observe that a point $\underline{T}$ of the *T-ellipsoid* can be defined as a linear function of $\underline{\alpha}$:

$$\underline{T} = \underline{T}(\underline{\alpha}) = [\underline{c}_x^T\underline{\alpha}, \underline{c}_y^T\underline{\alpha}, \underline{c}_z^T\underline{\alpha}, \underline{c}_{xx}^T\underline{\alpha}, \underline{c}_{yy}^T\underline{\alpha}, \underline{c}_{zz}^T\underline{\alpha}]^T \tag{11}$$

For instance, the components of $\underline{c}_x = [c_{1,x,x}, c_{2,x,x}, \dots, c_{n,x,x}, c_{1,y,x}, c_{2,y,x}, \dots, c_{n,y,x}, c_{1,z,x}, c_{2,z,x}, \dots, c_{n,z,x}]^T$, which has dimension 3n, are equal to $c_{i,k,x} = \sum_l Q_{i,k,x}^l$. The proof is straightforward and is omitted for brevity. This means that $c_{i,k,x}$ is the total horizontal force (for all the nodes, indicated by the index *l*) in the *x* direction, for the mode *i* and due to an earthquake in the direction k.

Let us now consider one of the 384 (or 1920) known vertices of the polyhedron enveloping the *T-ellipsoid*. We name this vertex $\underline{A} = [a_x, a_y, a_z, a_{xx}, a_{yy}, a_{zz}]^T$. Then, it is possible to prove that the point $\underline{B} = \underline{A} \Big/ \sqrt{\underline{A}^T \underline{\underline{X}}^{-1} \underline{A}} = [b_x, b_y, b_z, b_{xx}, b_{yy}, b_{zz}]^T$ lies on the surface of the *T-ellipsoid*. Moreover, $\underline{B}$ is the intersection between the *T-ellipsoid* and the segment linking the origin and the point $\underline{A}$. As a consequence, the problem that we have to solve can be written as follows:

$$\text{Find } \underline{\alpha} \text{ such that } \quad \underline{\alpha}^T \underline{\underline{\tilde{H}}}^{-1} \underline{\alpha} = 1 \quad \text{and} \quad \underline{T} = \underline{T}(\underline{\alpha}) = \underline{B} \tag{12}$$

This means that $\underline{\alpha}$ must be a point of the α-ellipsoid (of dimension 3n) and $\underline{T}(\underline{\alpha})$ must be a point of the 6D hyper-ellipsoid of the total forces and moments (*T-ellipsoid*). Notice that if a point $\underline{T} = \underline{T}(\underline{\alpha})$ belongs to the *T-ellipsoid* defined by the equation $\underline{T}^T \underline{\underline{X}}^{-1} \underline{T} = 1$, the point $\underline{T}' = \underline{\underline{X}}^{-1/2} \underline{T}$ belongs to a unit hyper-sphere defined by the equation $\underline{T}'^T . \underline{T}' = \left(\underline{\underline{X}}^{-1/2}\underline{T}\right)^T \left(\underline{\underline{X}}^{-1/2}\underline{T}\right) = \underline{T}^T \underline{\underline{X}}^{-1} \underline{T} = 1$. Consider two points on the surface of the unit hyper-sphere: $\underline{T}' = \left(\underline{\underline{X}}^{-1/2}\underline{T}\right)$ and $\underline{B}' = \left(\underline{\underline{X}}^{-1/2}\underline{B}\right)$. It is evident that $\underline{T}'\underline{B}' = \left(\underline{\underline{X}}^{-1/2}\underline{T}\right)^T \left(\underline{\underline{X}}^{-1/2}\underline{B}\right) = \underline{T}^T \underline{\underline{X}}^{-1} \underline{B} \le 1$ (Figure 4), the equality occurs when $\underline{T} = \underline{T}(\underline{\alpha}) = \underline{B}$. Hence, the solution $\underline{\alpha}$ of the problem in Equation 12 is also the solution of the following optimization problem:

$$\text{Find } \underline{\alpha} \text{ such that } \quad \underline{\alpha} = ARG\left(\max_{\forall \underline{\alpha} : \underline{\alpha}^T \underline{\underline{\tilde{H}}}^{-1} \underline{\alpha} = 1} \left[\left(\underline{T}(\underline{\alpha})\right)^T \underline{\underline{X}}^{-1} \underline{B} \right]\right) \tag{13}$$

According to the Lagrange multiplier method, the problem in Equation 13 is equivalent to:

Find $\underline{\alpha}$ such that $\underline{\alpha} = ARG\left(\max_{\forall \underline{\alpha}} \left[\left(\underline{T}(\underline{\alpha})\right)^T \underline{\underline{X}}^{-1} \underline{B} + \lambda\left(\underline{\alpha}^T \underline{\underline{\tilde{H}}}^{-1} \underline{\alpha} - 1\right)\right]\right)$. This leads to:

$$\lambda = \pm \frac{1}{2}\sqrt{\underline{c}^T \underline{\underline{\tilde{H}}}\underline{c}} \quad \text{and} \quad \underline{\alpha} = \pm \frac{\underline{\underline{\tilde{H}}}\underline{c}}{\sqrt{\underline{c}^T \underline{\underline{\tilde{H}}}\underline{c}}} \tag{14a \& 14b}$$

where $\underline{c} = \left[\underline{c}_x, \underline{c}_y, \underline{c}_z, \underline{c}_{xx}, \underline{c}_{yy}, \underline{c}_{zz}\right] \underline{\underline{X}}^{-1} \underline{B}$. The vector $\underline{\alpha}_A$ corresponding to the point $\underline{A}$ on the polyhedron reads $\underline{\alpha}_A = \underline{\alpha}\sqrt{\underline{A}^T \underline{\underline{X}}^{-1} \underline{A}}$. Each vector $\underline{\alpha}_A$ can be introduced into Equation 10 in order to define a static load field to be applied to the nodes of the structural model. Actually, there are 384 (or 1920) points $\underline{A}$, thus 384 (or 1920) vectors $\underline{\alpha}_A$ and 384 (or 1920) static load cases. All these load cases reproduce some probable combinations of the three total seismic forces and three moments at the building basis.

Figure 4. Points $\underline{T}$ and $\underline{B}$, $\underline{T}$' and $\underline{B}$' on the surfaces of the *T-ellipsoid* and the unit hyper-sphere.

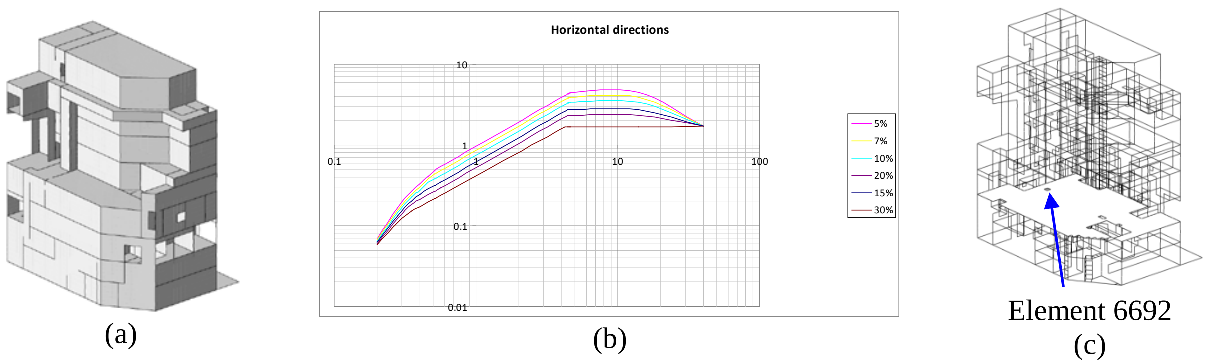

Figure 5. (a) Finite element model. (b) Pseudo-acceleration spectrum in horizontal directions (acceleration (m/s^2) vs. frequency (Hz)). (c) Finite element considered in Figure 6

4. APPLICATION TO A NPP REINFORCED CONCRETE BUILDING

In this Section, a comparison of four approaches with eight different procedures (or sub-approaches) for the seismic analysis of a NPP reinforced concrete building will be performed:

1. Complete Quadratic Combination of the modal shell efforts for each direction and Quadratic Combination of three directions (1st procedure: **CQC-Quadratic Combination**), 64 Combinations;
2. Complete Quadratic Combination of the modal shell efforts for each direction and Newmark's Combinations of three directions (2nd procedure: **CQC-24 Newmark's Combinations**);
3. Hyper-ellipsoid envelope of simultaneous shell efforts in each element of the model, i.e. $\underline{x} = \left[N_{xx}, N_{yy}, N_{xy}, M_{xx}, M_{yy}, M_{xy}\right]^T$ according to the notation of Section 1.2, where (N_{xx}, N_{yy}, N_{xy}) are membrane efforts and (M_{xx}, M_{yy}, M_{xy}) are bending moments. The approximation of the ellipsoids is carried out using three procedures defined in Section 2: polyhedron 384 vertices (3rd procedure: **Ellipsoid 384 points**), polyhedron 1920 vertices (4th procedure: **Ellipsoid 1920 points**) and intersection between two parallelepipeds (5th procedure: **Ellipsoid intersection 2 parallelepipeds**);
4. Static load cases using modal linear combinations and considering 384 (6th procedure: **Equivalent static 384 points, forces at the basis**) and 1920 (7th procedure: **Equivalent static 1920 points, forces at the basis**) probable combinations of three total forces and three total moments at the base of the structure (see Section 3). Another variant considering 384 probable combinations of three total forces and three total moments at each level of the structure is also studied (8th procedure: **384 points, forces at 6 levels**).

4.1. Structure description and modal analysis

Let us consider a reinforced concrete building with the following dimensions: width 16.5m, length 27.5m, height 31.94m (Figure 5a). The finite element software used for the structural analysis is HERCULE. The number of nodes and elements is 14400 and 16900, respectively. The soil under the foundation raft is modeled by a set of vertical and horizontal linear elastic springs. After the modal analysis, 35 modes plus the pseudo-mode are retained (n=36). A spectrum analysis is then carried out using the pseudo-acceleration spectrum of Figure 5b. For the earthquake in vertical direction, the spectrum ordinate is reduced by a factor equal to 2/3. The load cases used in this example include the permanent load (G) and the seismic load due to earthquakes in directions x, y and z.

4.2. Comparison of four approaches of seismic effort calculation

Once the efforts are known for each element of the model, the longitudinal reinforcement can be determined using the method proposed by Capra and Maury (1978), which provides the required reinforcement area (cm²/m) for both directions and for both upper and bottom layers of each shell element. The total reinforcement volume is estimated by summing the required reinforcement volumes of all shell elements, considering their sizes. Table 5 gives the ratios of the total reinforcement volumes found by the eight procedures, considering the "CQC-Newmark's Combinations" as reference method. One observes that the result obtained using the polyhedron enveloping the peak modal response hyper-ellipsoid (procedures 3 and 4) is very close to the reference one. The approximation by the intersection of 2 parallelepipeds (procedure 5) produces a considerable margin. The reinforcement volume obtained by the static load cases (6th procedure) is more important than the reference one. However, the result is less conservative with the finer approximation of the 7th procedure. The difference between this approach and the hyper-ellipsoid envelope can be explained by the fact that the 6-dimension *T-ellipsoid* is discretized by a polyhedral envelope which is larger than the original *T-ellipsoid*. As expected, the "CQC-Quadratic Combination" (procedure 1) gives the maximum reinforcement demand.

Table 5: Comparison of the eight procedures of seismic analysis in terms of reinforcement quantity

Approach	Procedure		Total reinforcement ratio
1	CQC-Quadratic Combination (1)		1.58
2	CQC-Newmark's Combinations (2)		1.00
3	Hyper-ellipsoid response envelope	Ellipsoid 384 points (3)	0.99
		Ellipsoid 1920 points (4)	0.97
		Ellipsoid intersection 2 parallelepipeds (5)	1.09
4	Equivalent static loads	384 points, forces at the basis (6)	1.14
		1920 points, forces at the basis (7)	1.05
		384 points, forces at six levels (8)	1.20

The difference between the four approaches – eight procedures can also be illustrated by plotting the points representing the combinations of the six efforts $N_{xx}, N_{yy}, N_{xy}, M_{xx}, M_{yy}, M_{xy}$, in one shell element of the structure. A 6D space should be considered. For the finite element indicated in Figure 5c, the projections of these efforts in the plane $N_{xx} - N_{yy}$ are shown in Figure 6.

Figure 6 shows that (i) the points obtained by the "equivalent static load" approach, especially when several levels of the building are considered (procedure "Equivalent static 384 points, six levels"), envelope almost all the points of the hyper-ellipsoid envelope of shell efforts and the CQC-Newmark's points. That explains why the reinforcement demand found by the "equivalent static" approach is more important than the ones found by approaches 2 and 3; (ii) the reinforcement quantity obtained by the "CQC-Quadratic Combinations" is the most important. The efforts are strongly overestimated especially when an important correlation between shell efforts exists; (iii) for the "hyper-ellipsoid response envelope" and "equivalent static loads" approaches, the reinforcement quantity is reduced when using a finer approximation (approximation with 1920 points); (iv) the approximation of the hyper-ellipsoid by the intersection of the two enveloping parallelepipeds gives conservative results.

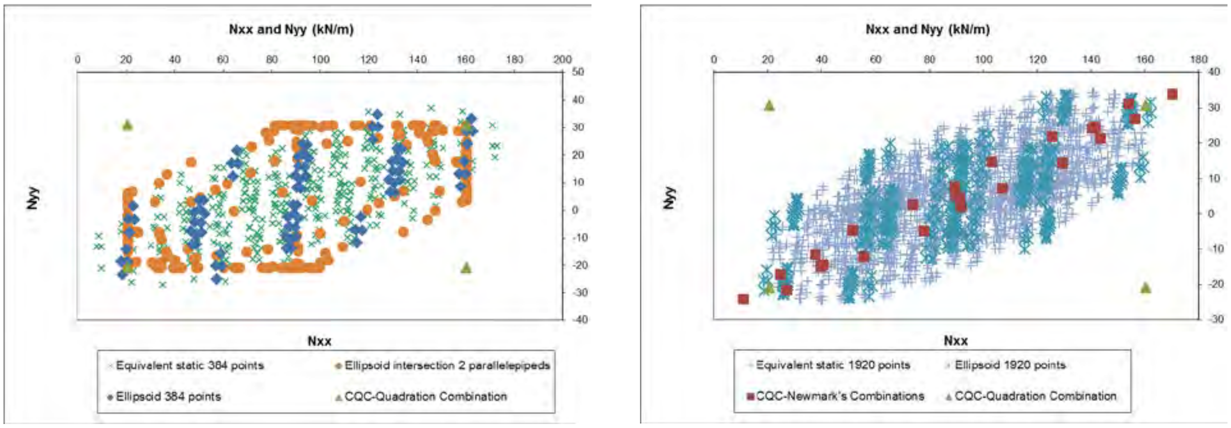

Figure 6. $N_{xx} - N_{yy}$: seismic efforts obtained by the eight procedures of Table 5

5. CONCLUSIONS

In the first part of the paper, the definition of the peak hyper-ellipsoid response envelope has been recalled. Several methods for the discretization of this hyper-ellipsoid are mentioned and studied in depth. An improvement of the classical discretization technique has been proposed. The definition of equivalent static load cases based on the hyper-ellipsoid envelopes has been presented in Section 3. In Section 4, four variants (approaches) – eight procedures of the response spectrum method have been applied on a NPP building. The comparisons in terms of total reinforcement volume and in terms of efforts in a shell element demonstrate the advantages of the novel ellipsoid discretization approach developed in Section 2. All procedures presented here are easy-to-implement and applicable in practical calculation.

REFERENCES

Martin, F. (2004). "Problèmes de concomitance en analyse modale spectrale. Combinations linéaires de modes – Domaine de concomitance". *Internal report – IOSIS Industries* (in French).

Nguyen, Q.S., Erlicher, S. and Martin, F. (2012). "Comparison of several variants of the response spectrum method and definition of equivalent static loads from the peak response envelopes", *15th World Conference of Earthquake Engineering.* **September 2012,** *paper 4269*.

Vézin, J-M., Martin, F., Langeoire, A. and Cazadieu, S. (2007). "Optimisation du dimensionnement sismique par analyse spectrale en utilisant le domaine de concomitance des sollicitations" . *Colloque AFPS 2007* (in French).

Menun, C. and Der Kiureghian, A. (2000a&b). "Envelopes for seismic response vectors. I: Theory. II: Application". *Journal of structural* engineering. **April 2000**, 467-473.

Leblond, L. (1980). "Calcul sismique par la méthode modale. Utilisation des réponses pour le dimensionnement". *Théories et méthodes de calcul* **N°380**, 119-127 (in French).

Der Kiureghian, A. (1979). "On reponse of structures to stationary excitation". *Earthquake Engineering Research Center. University of California, Berkeley*. Report No. UCB/EERC-79/32.

ASCE 4-09 (2009). Working *Group* on Revision of ASCE Standard 4. Seismic analysis of safety-related nuclear structures, Draft.

Capra, A. and Maury, J.F (1978). "Calcul automatique du ferraillage optimal des plaques ou coques en béton armé". Annales de l'insitut technique du bâtiment et des travaux publics. N° 367 (in French).